AIRS Version 6
Level 2 Cloud Cleared Radiances

Edited by:
Edward T. Olsen

Contributions by:
Joel Susskind, GSFC, John Blaisdell, Lena Iredell, SAIC/GSFC
Goddard Space Flight Center, NASA

February 2013
Version 1.0

Jet Propulsion Laboratory
California Institute of Technology
Pasadena, CA

Submit Questions to:
 http://airs.jpl.nasa.gov/AskAirs

Table of Contents

Table of Figures

1   Overview

The general methodology used to analyze AIRS+AMSU observations in both Version-5 (V5) and Version-6 (V6) is essentially unchanged from that described in Susskind et al. (2003). More details about the AIRS V6 retrieved methodology are given in the AIRS V6 ATBD. Fundamental to this approach is the generation of clear column radiances for each AIRS channel i, $\widehat{R}_i$, which are derived products representing the radiance channel i would have seen if the entire 3x3 AIRS Field of Regard (FOR) on which a retrieval is performed were cloud free. $\widehat{R}_i$ is determined for each channel as a linear combination of the observed radiances of that channel in each of the 9 AIRS Fields of View (FOV's) contained within the AIRS FOR, using coefficients that are channel independent (Susskind et al., 2003). The retrieved geophysical state X is subsequently determined which, when substituted in a Radiative Transfer Algorithm (RTA), generates an ensemble of computed radiances $R_i(X)$ which are consistent with $\widehat{R}_i$ for those channels i used in the determination of X. Aside from being an integral part of the retrieval process, $\widehat{R}_i$ can also be potentially used in data assimilation experiments and also for process studies. $\widehat{R}_i$ are also sometimes referred to as cloud-cleared radiances.

The AIRS clear column radiances require quality control for optimal use in data assimilation or validation studies. V4 had a single case dependent Qual_CCR_flag, which is NOT adequate, as it provides no distinction among channels. V6 has a separate case dependent Qual_CCR_flag for each channel, based on thresholds of the case dependent clear column radiance error estimate $\delta\widehat{R}_i$. The V6 methodology used to generate $\delta\widehat{R}_i$ was designed to accommodate the assimilation of $\widehat{R}_i$ as a part of a data assimilation scheme. The most important channels for radiance assimilation purposes are in the longwave temperature sounding spectral region 650 cm^{-1} – 740 cm^{-1}, and the error estimate methodology was designed primarily for use in this spectral region. In V6, error estimates are provided in each retrieval for each channel. This information is provided in the DISC "L2 Standard Cloud-Cleared Radiance Product" dataset as the word radiance_err. Each channel also has a case dependent Quality flag, 0, 1, or 2, based on thresholds of $\delta\widehat{R}_i$. These channel by channel QC flags are written for all channels in the word radiances_QC. Clear column radiances in channels with QC=0 for a given retrieval case are considered to have the highest accuracy, and are recommended for potential use in data assimilation experiments. Clear column radiances in channels with QC=1 are considered to be of good quality and are recommended for inclusion in other applications, such as process studies. Clear column radiances in channels with QC=2 are not recommended for scientific use.

2 Error Estimates for $\widehat{R}_i$

The clear column radiance for channel i, $\widehat{R}_i$, is a derived quantity obtained as part of the V6 physical retrieval process, and, like other derived quantities, has an associated case and channel dependent error estimate $\delta\widehat{R}_i$. Values of $\widehat{R}_i$ and $\delta\widehat{R}_i$ are generated for all operable AIRS channels in those cases where a successful IR/MW retrieval is produced (roughly 99% of all cases). The AIRS+AMSU V6 retrieval algorithm performs one retrieval per AMSU FOR, which contains 9 AIRS FOV's. Each AIRS FOV (j = 1,9) within the AMSU FOR has an observed radiance for each channel i, $R_{i,j}$. The observations $R_{i,j}$ are potentially affected by clouds in FOV j. $\widehat{R}_i$ represents the best estimate of what the observed AIRS channel i radiance, averaged over the 9 FOV's in the AMSU FOR, would have been if all FOV's were completely cloud free. $\widehat{R}_i$ is obtained according to

$$\widehat{R}_i = \overline{R}_i + \sum_{j=1}^{9} \eta_j \left(\overline{R}_i - R_{i,j} \right) \tag{1}$$

where $\overline{R}_i$ is the average value of $R_{i,j}$ over the 9 FOV's and η_j (j=1,9) is a derived vector for each FOR obtained as part of the retrieval process. The physical retrieval process finds the surface and atmospheric state X such that radiances computed using X best match the derived clear column radiances $\widehat{R}_i$. $\widehat{R}_i$ can also be used as input for data assimilation purposes. For optimal results, data assimilation should take into account $\delta\widehat{R}_i$ to decide which values of $\widehat{R}_i$ should be assimilated on a case-by-case basis.

If all values of η_j used in Equation 1 were perfect, then the error in $\widehat{R}_i$ would be

$$\delta\widehat{R}_i^{per} = \widetilde{A}\ NE\Delta N_i \tag{2}$$

where $NE\Delta N_i$ is the spatially random noise of channel i and where $\widetilde{A}$ is the channel noise amplification factor, resulting from taking the linear combination of observations in the nine FOV's, shown in Equation 1, to obtain $\widehat{R}_i$. It can be shown that the appropriate value of $\widetilde{A}$ is given by

$$\widetilde{A} = \left[\left(\sum_{j=1}^{9} \frac{1}{9} \cdot \left(1 + \sum_{j'=1}^{9} \eta_{j'} \right) - \eta_{j} \right)^{2} \right]^{1/2} \tag{3}$$

Equation 1 shows that $\widehat{R}_i = \overline{R}_i$ if all $\eta_j's$ are zero. This situation corresponds to a case in which the clear column radiance is obtained by averaging the radiances in all nine FOV's. Equation 3 reduces to $\widetilde{A} = 1/3$ when all $\eta_j's$ are zero. In general, this is not the case and $\widetilde{A}$ is usually greater than 1, depending on the extent of cloud clearing (extrapolation) performed in the FOR.

$\widetilde{A}$ is in principle channel independent because it arises only from the linear combination of radiances used to construct $\widehat{R}_i$. Some channels are only sensitive to the atmosphere at pressures sufficiently lower than the cloud top pressure (altitudes higher than the cloud top height), and these case dependent channels do not "see" the clouds. The retrieval algorithm determines which channels do not "see" clouds, and for these channel sets $\widehat{R}_i = \overline{R}_i$ and also sets $\widetilde{A} = \widetilde{A}^{CLR} = 1/3$ for such channels. Equation 3 is used for $\widetilde{A}_i$ for all other channels.

In general, the largest source of noise in $\widehat{R}_i$ results from errors in the vector η_j. In V6, as we did in V5, we express $\delta\widehat{R}_i$ as the sum of the errors arising from both sources, $\delta\widehat{R}_i^{per}$ and $\delta\widehat{R}_i^{\delta\eta}$, where $\delta\widehat{R}_i^{\delta\eta}$ according to

$$\delta\widehat{R}_i^{\delta\eta} = \sum_{k=1}^{7} M_{i,k}^{R} \delta Y_k \tag{4}$$

The first 6 predictors δY_k used in Equation 4 are the case-by-case error estimates (K) of the retrieved temperature profile at 150 hPa, 260 hPa, 500 hPa, 700 hPa, 850 hPa, and 1000 hPa, and the last predictor is the fractional error estimate (%) of retrieved total precipitable water. In general, the case-by-case clear column radiance error estimate $\delta\widehat{R}_i$ is computed according to the sum of the two sources of noise

$$\delta\widehat{R}_i = \widetilde{A}_i \, NE\Delta N_i + \left| \sum_{k=1}^{7} M_{i,k}^{R} \, \delta Y_k \right|. \tag{5a}$$

If all 9 values of $R_{i,j}$ were unaffected by clouds, then for channel i, $\widehat{R}_i$ would be best approximated by $\overline{R}_i$, and $\delta\widehat{R}_i$ for that channel is given by

$$\delta\widehat{R}_i = 1/3\ NE\Delta N_i \qquad\qquad (5b)$$

Equation 5b is used for $\delta\widehat{R}_i$ for all FOR's in which $\widetilde{A}_i = 1/3$ for channel i.

3 Clear Column Brightness Temperature $\widehat{\varTheta}_i$

Clear column radiances and their associated error estimates are written out in radiance units (W/m^2-sr-cm^{-1}). It is more convenient, however, to think in terms of clear column brightness temperatures $\widehat{\Theta}_i$, and their error estimates $\delta\widehat{\Theta}_i$, both given in K. The clear column brightness temperature $\widehat{\Theta}_i$ is defined as the equivalent blackbody temperature of $\widehat{R}_i$, and is the temperature such that $B(v_i, \widehat{\Theta}_i) = \widehat{R}_i$ where $B(v_i, T)$ is the Planck blackbody function. Given $\widehat{R}_i$ and $\delta\widehat{R}_i$, $\delta\widehat{\Theta}_i$ is evaluated according to

$$\delta\widehat{\Theta}_i = \delta\widehat{R}_i \left(\frac{dB(v_i, T)}{dT}\right)^{-1}_{\widehat{\Theta}_i} \qquad\qquad (6)$$

There are six different matrices MR used in Equation 5a for each of six different spatial and temporal domains. There are separate matrices M for use under daytime and nighttime conditions over each of non-frozen ocean, land, and snow and ice, which were determined once and for all based on observations on September 29, 2004 and February 24, 2007. The coefficients of the six different matrices MR were determined using coefficients $M^R_{i,k}$ that minimize the RMS differences of $(\delta\widehat{\Theta}_i - \Delta\widehat{\Theta}_i)$ where $\Delta\widehat{\Theta}_i = (\widehat{\Theta}_i - \Theta_i^{truth})$ and $\delta\widehat{\Theta}_i$ is computed using Equations 5a and 6. The true clear column brightness temperature, Θ_i^{truth}, is the value of Θ_i that is computed using the AIRS RTA in conjunction with a truth state Xtruth. We used ECMWF 3-hour forecast values for $T_{skin}^{truth}, T(p)^{truth}, q(p)^{truth}$, and $O(p)_3^{truth}$. The CO_2^{truth} profile used in the calculations had a spatially homogeneous vertically constant mixing ratio which was set to be 371.79 ppm on January 1, 2002, and increased linearly in time at a rate of 2.026 ppm/yr. The truth values used for CO(p), CH4(p), and N2O(p) were based on spatially varying monthly mean climatologies. The AIRS Team model was used as truth for surface emissivity over non-frozen ocean. Reasonable globally homogeneous surface emissivity values were used as truth over land. Values of Θ_i^{truth}, and therefore of $\Delta\widehat{\Theta}_i$, are most accurate for channels in the 15 µm and 4.3 µm CO2 bands, especially those channels which are less sensitive to surface emission. For this reason, the best error estimate coefficients and error estimates are

generated in the 15 μm and 4.3 μm CO2 bands for those channels which are not sensitive to surface emission. Error estimate coefficients generated for channels which are very sensitive to water vapor or ozone absorption are less accurate because of limitations in the truth values used for water vapor and ozone profiles. Error estimate coefficients for those channels which are very sensitive to surface emission are also less reliable, but are better over ocean than over land. Finally, clear column radiances at frequencies greater than or equal to 2175 cm^{-1} are affected by incoming solar radiation reflected by the surface back in the direction of the satellite. The relevant surface bi-directional reflectance term ρ_i is not modeled well in the computation of Θ_i^{truth}. For this reason, daytime values of $M_{i,k}^R$ for frequencies between 2180 cm^{-1} and 2240 cm^{-1}, and between 2380 cm^{-1} and 2660 cm^{-1}, are of lower accuracy because radiances in these channels are sensitive to reflected solar radiation which is not well modeled in Θ_i^{truth}. Therefore, we substituted the values of $M_{i,k}^R$ determined during nighttime conditions for these channels, in place of those that were computed during daytime conditions, in the daytime matrices of M^R.

4 QC flags for $\widehat{R}_i$

Different channels are sensitive, by varying amounts, to clouds at different pressures. Therefore, $\delta\widehat{\Theta}_i$ is both channel and case dependent. Even if significant cloud clearing errors exist for some channels in a given case, channels that have little or no sensitivity to the clouds in that case would have very accurate values of $\widehat{R}_i$. It is for this reason that we assign each channel its own case dependent QC flags indicating whether the cloud-cleared radiance $\widehat{R}_i$ is of sufficient accuracy for use for different purposes. We used the predicted clear column brightness temperature error $\delta\widehat{\Theta}_i$ to assign the QC flags for $\widehat{R}_i$ on a case-by-case basis. $\widehat{R}_i$ is assigned the flag QC=0 if $\delta\widehat{\Theta}_i$ is less than 1.0K, and is assigned the QC flag QC=1 if $\delta\widehat{\Theta}_i$ is between 1.0K and 2.5K. Otherwise, the QC flag is set equal to 2. The flag QC=0 is intended to mark those channels that are thought to be accurate enough for data assimilation purposes, with the goal that the error in $\widehat{R}_i$ should be not much larger than the channel noise $NE\Delta N_i$. The flag QC=1 is designed to provide a better spatial coverage for a given scene but still eliminate poor values of $\widehat{R}_i$.

Figure 1 shows the spatial coverage and accuracy of Quality Controlled values of $\left(\widehat{\Theta}_i - \Theta_i^{truth}\right)$ at 715.94 cm^{-1} and at 724.52 cm^{-1} for the 1:30 PM orbits on September 29, 2004. These channels have peak atmospheric sensitivity to temperatures at 461 hPa and 580 hPa, respectively. Figure 1a shows that the spatial coverage of $\widehat{R}_i$ at 715.94 cm^{-1} (461 hPa) with QC=0 is almost complete with small gaps in a few areas. The global mean standard deviation of $\left(\widehat{\Theta}_i - \Theta_i^{truth}\right)$ for these cases is 0.70K, which is not appreciably higher than the noise for this channel. When the Quality Control for this channel is relaxed to allow cases with QC=0 or 1, as shown in Figure 1b, there is almost complete

spatial coverage, and the standard deviation of $\left(\widehat{\Theta}_i - \Theta_i^{truth}\right)$ for these cases increases, but only to 0.94K. Analogous results for 724.52 cm^{-1} (580 hPa) show somewhat lower yields and larger errors, because this channel is more sensitive to lower clouds.

Figure 1: Spatial coverage and accuracy of L2 cloud cleared radiances for two channels

Left: QC = 0   Right: QC = 0,1
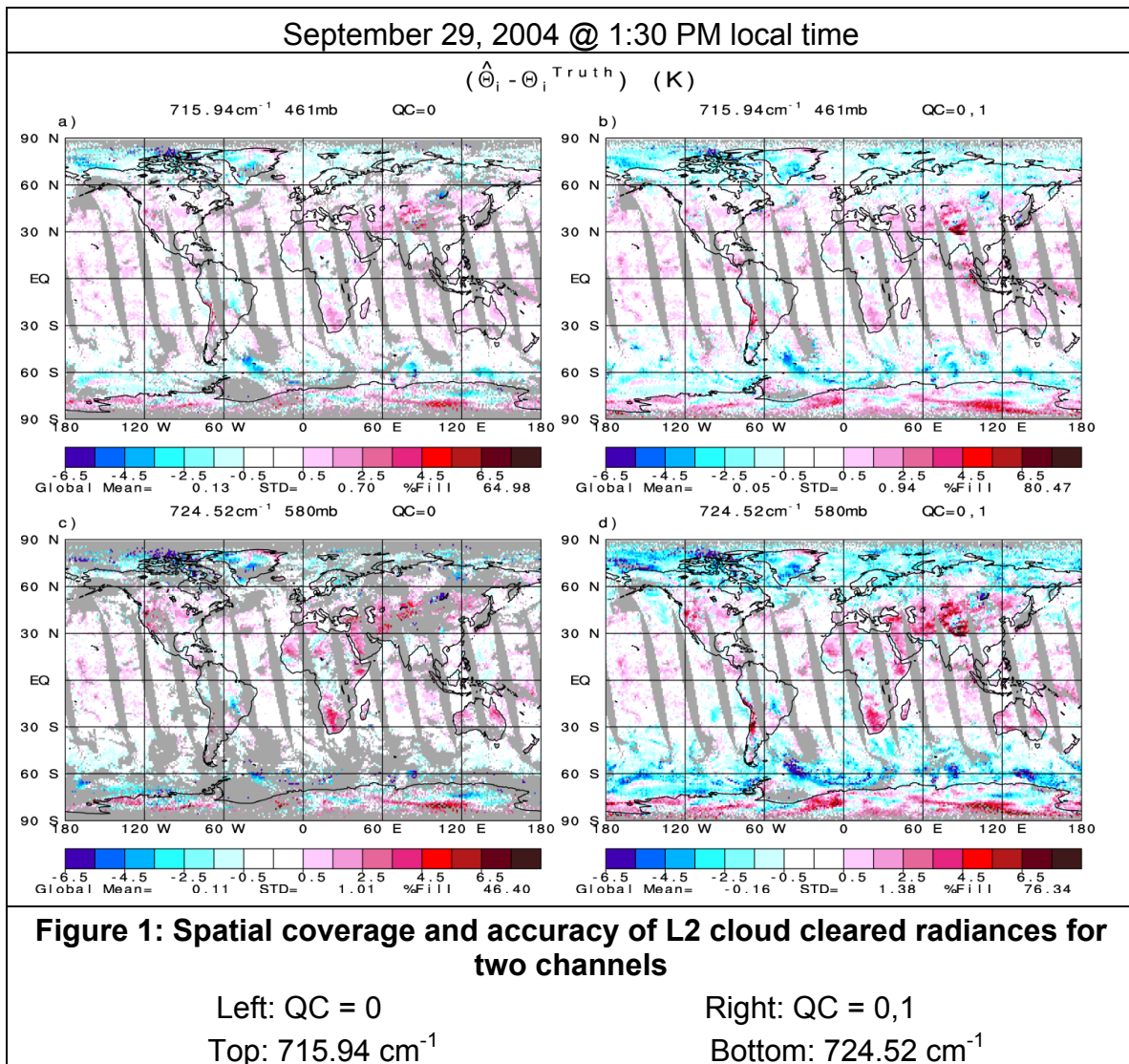
Top: 715.94 cm^{-1} Bottom: 724.52 cm^{-1}

Figure 2a shows the spatial distribution of V6 values of cloud fraction αε and cloud top pressure pc for the 1:30 PM orbits of September 29, 2004. This plot depicts both αε and pc at the same time. There are seven different color scales used for different intervals of pc, as indicated on the figures. Reds and violets and purples indicate high clouds, blues and greens indicate mid-level clouds, and oranges and yellows indicate low clouds. Within each color scale, darker colors indicate larger fractional cloud cover, and paler colors indicate low fractional cloud covers. It is apparent that the small gaps in Figure 1a correspond to areas where large amounts of mid-high level clouds, depicted in dark purple in Figure 2a, exist. The somewhat larger gaps in spatial coverage in Figure 1c include additional areas of extensive cloud cover shown in greens and yellows in Figure 2a.

September 29, 2004 @ 1:30 PM local time

Figure 2: Spatial distribution of V6 cloud fraction and cloud top pressure, QC=0,1

Left: cloud top pressure (hPa)   Right: Surface Skin Temperature (K)
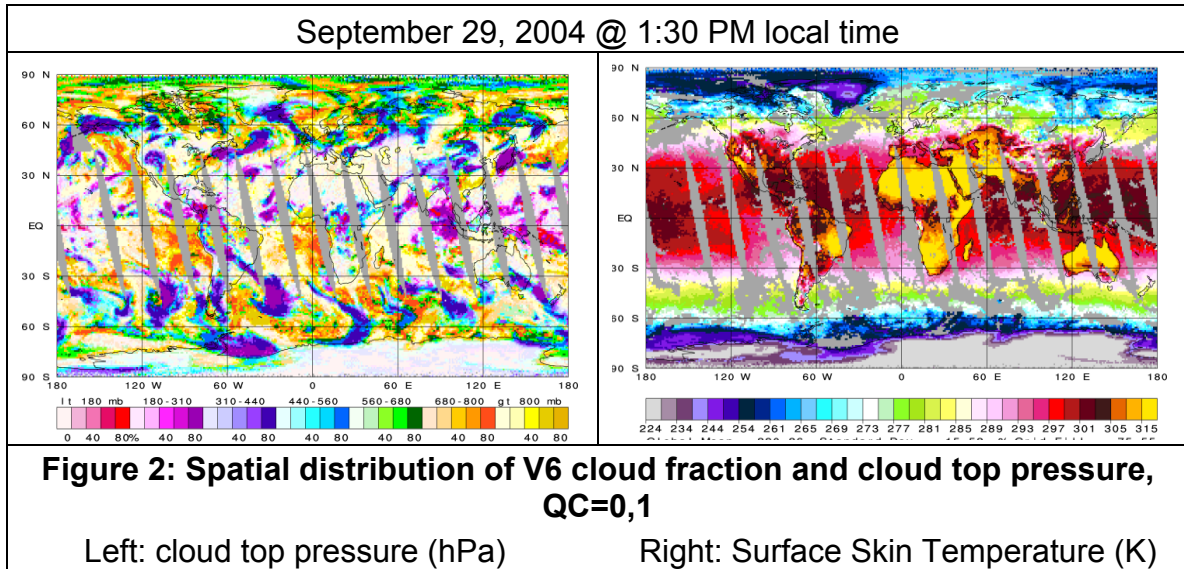
Figure 2b shows values of Tskin with QC=0 or 1 for the same set of orbits. Quality control for Tskin over ocean is much tighter than for Tskin over land because Tskin over ocean is known much better over ocean than over land. More details are given in the AIRS ATBD. The spatial coverage of Tskin over ocean with QC=0 or 1 is very extensive, but gaps exist in areas of extensive cloud cover, including areas of extensive stratus cloud cover, shown in dark oranges and yellows, off the west coasts of South America and Africa. The areas of gaps in coverage of Tskin over ocean contain those areas with gaps in coverage in $\widehat{R}_i$ at 724.52-1 with QC=0, shown in Figure 1c. Most of these gaps are filled in when QC for $\widehat{R}_i$ at 724.52-1 is relaxed to include cases with QC=1, but contain cases with relatively small spuriously low values of $\widehat{R}_i$. It is interesting to note that the red areas over land in Figures 1c and 1d, and to a lesser extent in Figures 1a and 1b, correspond to areas with very high values of Tskin during the day. The positive (red) differences in $\left(\widehat{\Theta}_i - \Theta_i^{truth}\right)$ in these areas are a result of the ECMWF values of Tskin not being warm enough, and consequently, Θ_i^{truth} being too low.

Figure 3 displays spectral characteristics of V6 AIRS+AMSU (**AIRI2CCF**) and V6 AIRS-Only (**AIRS2CCF**) (notation is "AO") clear column radiances with Quality Flags QC=0, and also with QC=0 or 1, over the 15 μm spectral domain 650 cm^{-1} through 740 cm^{-1}, for which the $\widehat{R}_i$ error estimate and QC methodology was primarily designed. The spectral locations of the two channels whose errors are shown in Figure 1 are indicated by thin red vertical lines. V6 **AIRI2CCF** results are shown in dark blue for the ensemble of cases with QC=0, and in light blue for cases with QC=0 or 1. V6 **AIRS2CCF** results are shown in black and

gray for the same sets of cases respectively. The results shown are for all global cases that were observed by AIRS over nine test days selected in different months and years. All results are shown in the brightness temperature domain.

Figure 3: Mean cloud-cleared radiance column brightness temperature, yield and bias 650 cm^{-1} to 740 cm^{-1} for V6, QC=0
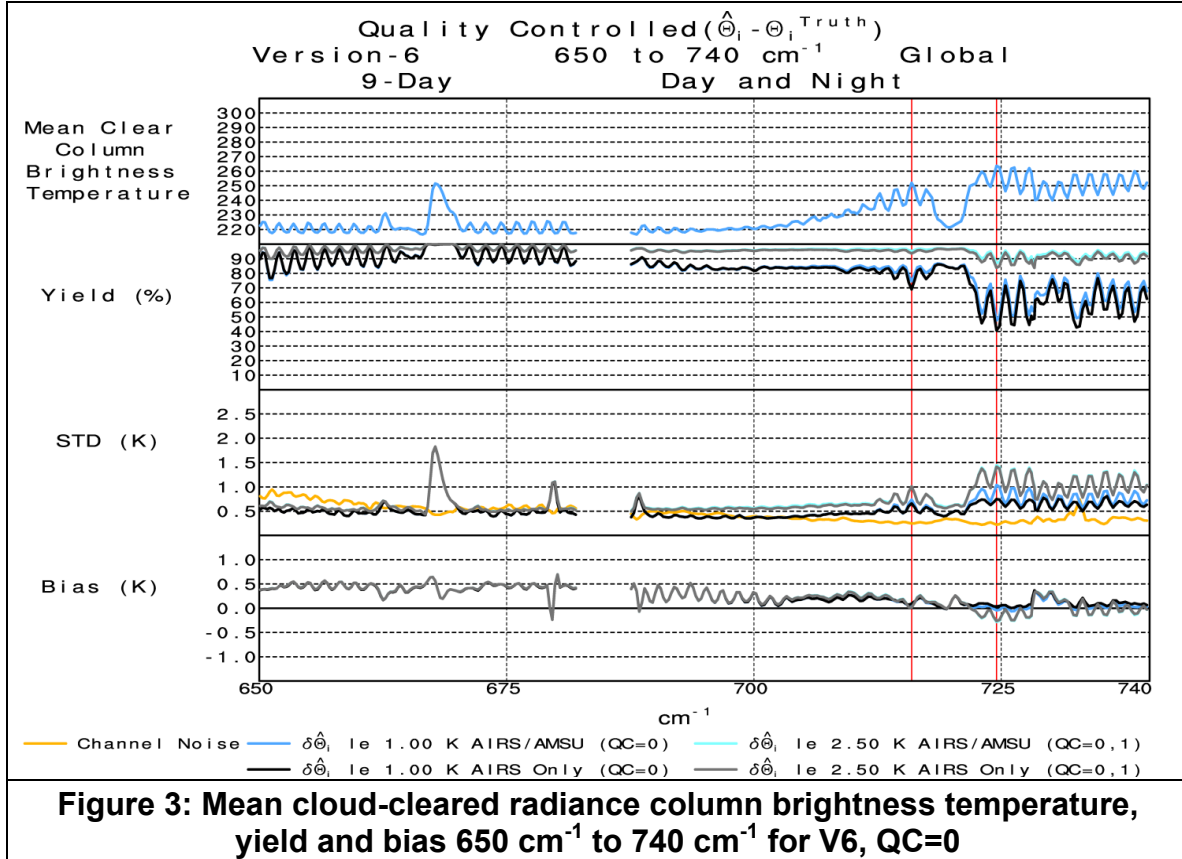
The top panel in Figure 3 shows the mean clear column brightness temperature spectrum of all cases with QC=0. The brightness temperature for a given channel corresponds to a weighted average temperature over the pressure interval which the channel radiance is sensitive to. The higher brightness temperatures occur in channels primarily sensitive to mid-lower tropospheric temperature. Channels at frequencies centered on absorption lines sense higher in the atmosphere than those off the corresponding lines, and therefore have lower brightness temperatures when sensing the troposphere, and higher brightness temperatures when sensing the stratosphere. The transition between the two domains occurs at roughly 710 cm^{-1}.

The second panel of Figure 3 shows the percentage of all FOV's in which $\widehat{\Theta}_i$ was found acceptable using the 1.0K and 2.5K criteria for $\delta\widehat{\Theta}_i$ in both V6 **AIRI2CCF** and V6 **AIRS2CCF**. Yields increase at lower frequencies, in which channels are

primarily sensitive to radiation emitted higher in the atmosphere, and hence are less sensitive to clouds in the field of view. For the same reason, yields are higher at frequencies located on absorption lines than those located off them, so yields are higher at frequencies with local minima of brightness temperatures when sensing the troposphere and are higher at frequencies with local brightness temperature maxima when sensing the stratosphere. Yields with QC=0,1 are higher than those with QC=0, especially as the channels become more sensitive to mid-lower tropospheric temperatures. The channels near 667 cm^{-1} are special cases, in that they are sensitive to temperatures in the pressure interval 1 hPa to 10 hPa, and are insensitive to any cloud cover. These channels have a 100% yield using either set of QC flags. There is essentially no difference in yields obtained with a given QC flag using either V6 **AIRI2CCF** or V6 **AIRS2CCF**.

The third panel in Figure 3 shows the standard deviations (STD) of the quality-controlled values of $\left(\widehat{\Theta}_i - \Theta_i^{truth}\right)$ in the same colors as used for yields. The yellow line shows the mean value of the channel noise $NE\Delta N_i$ in brightness temperature units when evaluated at $\widehat{\Theta}_i$. There is again essentially no difference in the results for V6 **AIRI2CCF** and V6 **AIRS2CCF** when the same QC procedure is used. It is interesting to note that the errors in $\Delta\widehat{\Theta}_i$ are less than or equal to the channel noise (yellow line) at frequencies lower than 710 cm^{-1} when using the ensemble of QC=0 cases. The reduction in noise for these stratospheric channels results from the ability to average the radiances observed over the 9 FOV's to obtain $\widehat{R}_i$, because these channels for the most part are unaffected by clouds. The standard deviations of the errors in $\widehat{\Theta}_i$ are larger using cases with QC=0,1, compared to QC=0, especially for channels more sensitive to lower tropospheric and surface skin temperatures. The increases in the standard deviation of the errors in $\widehat{\Theta}_i$ for these channels is partly a result of larger cloud effects on the radiances for those channels (errors in $\widehat{\Theta}_i$) and partly the result of a larger contribution of the surface in the computation of Θ_i^{truth} (errors in Θ_i^{truth}). Note for example the regions of positive differences over land in $\left(\widehat{\Theta}_i - \Theta_i^{truth}\right)$ shown in Figure 1, which have been discussed previously. The large standard deviations of the errors near 667 cm^{-1} are also an artifact arising from errors in ECMWF T(p) above 10 hPa.
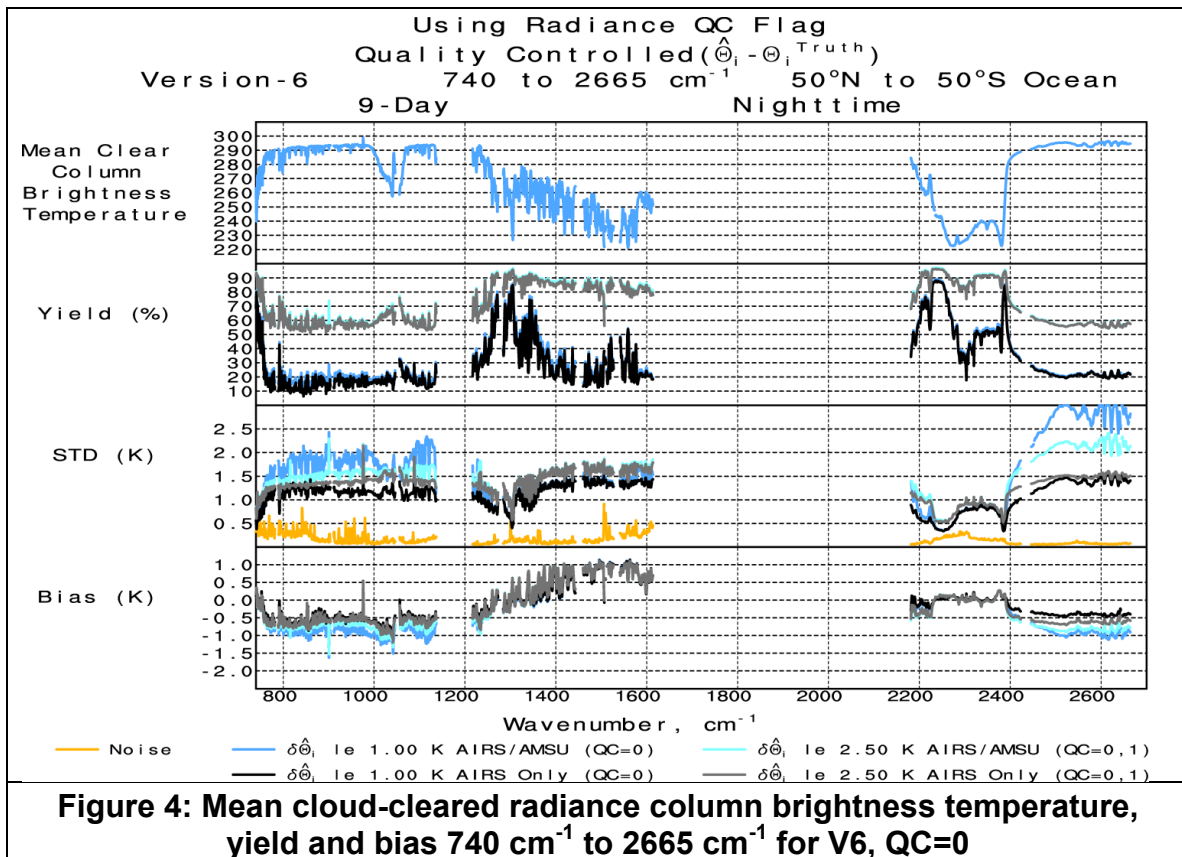
The lowest panel of Figure 3 shows the bias of the differences between $\widehat{\Theta}_i$ and Θ_i^{truth}. Again, there is essentially no difference between V6 **AIRI2CCF** and V6 **AIRS2CCF**. Part of these biases result from errors in the computation of Θ_i^{truth} due to both radiative transfer errors and errors in X^{truth}. For example, the positive biases, on the order of 0.5K, between $\widehat{\Theta}_i$ and Θ_i^{truth} found for channels sounding the stratosphere, are certainty not a result of cloud clearing errors.

Figure 4 is analogous to Figure 3 but shows results for the remaining spectral domain of AIRS, from 740 cm^{-1} to 2665 cm^{-1}. Much of this spectral domain contains window regions in which the observed radiances are sensitive primarily

to surface skin temperature and emissivity. Surface skin temperature and emissivity are much better characterized by ECMWF "truth" over ocean than over land. For this reason, the results shown in Figure 4 are only for ocean cases 50˚N – 50˚S latitude. In addition, during the day, radiances in shortwave channels sensitive to surface emission are also sensitive to incoming solar radiation reflected by the surface back to space in the direction of the satellite. The appropriate surface spectral bi-directional reflectance term is also not well characterized by ECMWF "truth". For this additional reason, Figure 4 shows results over ocean for nighttime cases (1:30 AM) only.

Figure 4: Mean cloud-cleared radiance column brightness temperature, yield and bias 740 cm^{-1} to 2665 cm^{-1} for V6, QC=0

Radiances between 1250 cm^{-1} and 1600 cm^{-1} are strongly influenced by water vapor absorption in the atmosphere. These water vapor lines increase in strength with increasing frequency up until about 1580 cm^{-1}. Channel brightness temperatures decrease both on and off H2O absorption lines as the H2O absorption line strengths intensify, because emission at these frequencies comes from water vapor at increasing altitudes. The QC procedure developed for use in the 15 μm CO2 band results in a significant drop in yield for cases with QC=0 compared to QC=0,1 in this spectral domain, with a relatively small drop in standard deviations of $\left(\widehat{\Theta}_i - \Theta_i^{\text{truth}}\right)$. The standard deviation results are

somewhat misleading however because a large source of the apparent "error" in $\widehat{\Theta}_i$ for these channels results from errors in the ECMWF water vapor profile, and hence errors in Θ_i^{truth}. There is essentially no difference between V6 **AIRI2CCF** and V6 **AIRS2CCF** in the yields and standard deviation of the "errors" in $\widehat{\Theta}_i$ using a given QC procedure. The same result holds for the biases between $\widehat{\Theta}_i$ and Θ_i^{truth}, which are shown in the fourth panel of Figure 4. These biases are also not indicative in the accuracy of $\widehat{\Theta}_i$ because they arise primarily from biases in Θ_i^{truth}.

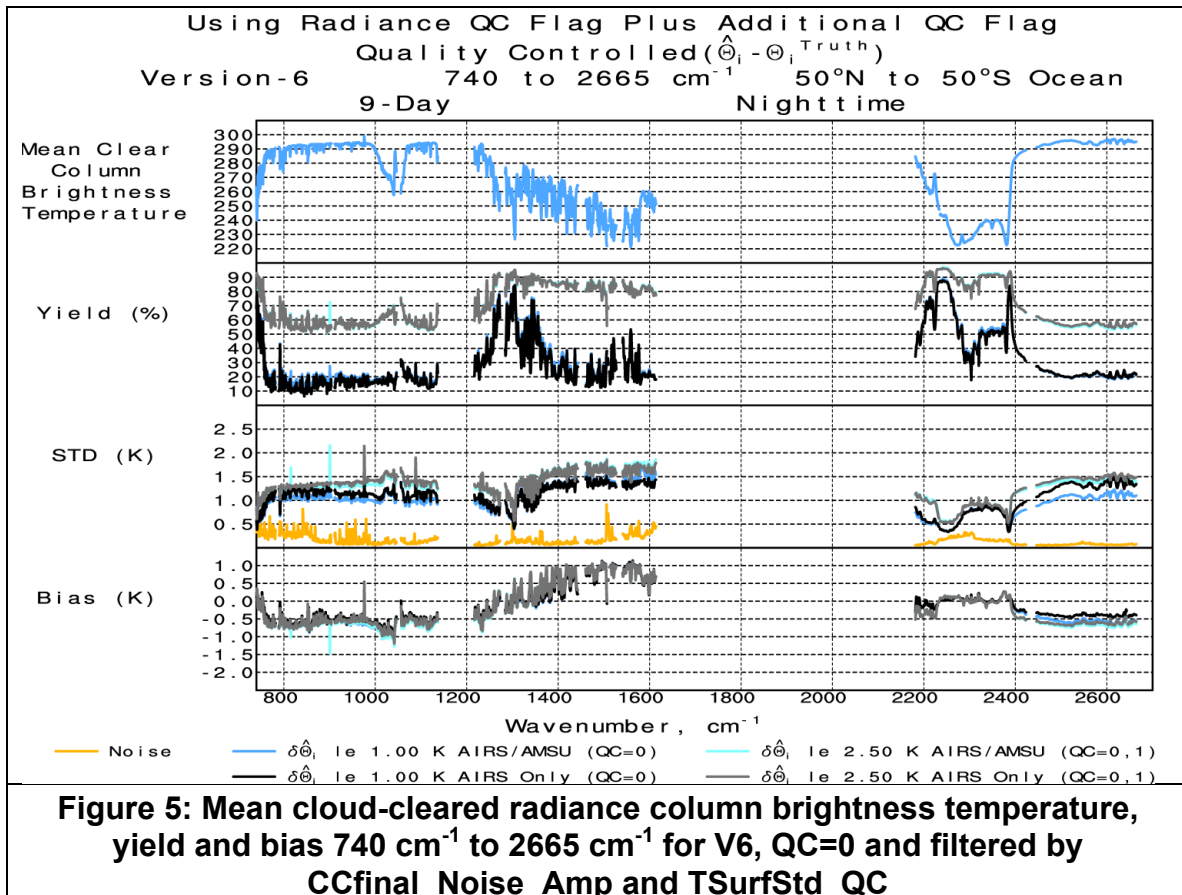The spectral intervals between 750 cm^{-1} and 1137 cm^{-1}, and between 2400 cm^{-1} and 2665 cm^{-1}, are window regions in which channel radiances are primarily sensitive to emission from the earth's surface and absorption and emission from the lower troposphere. In these spectral regions, yields of $\widehat{\Theta}_i$ are again virtually identical between V6 **AIRI2CCF** and V6 **AIRS2CCF** when analogous QC procedures are used. There is a very big difference, however, in the standard deviations of $(\widehat{\Theta}_i - \Theta_i^{truth})$, as well as their biases, between the results found in V6 **AIRI2CCF** and V6 **AIRS2CCF**. These results are doubly counter-intuitive in that: 1) V6 **AIRI2CCF** standard deviations, as well as negative biases, are both considerably larger than those of V6 **AIRS2CCF**, and 2) the results of V6 **AIRI2CCF** with QC=0 are considerably poorer than those with QC=0,1.

These counter-intuitive and very poor results arise from a logical flaw in the methodology used to generate $\delta\widehat{R}_i$ (and consequently $\delta\widehat{\Theta}_i$) when applied to window channels, especially over ocean. Under most conditions, $\delta\widehat{R}_i$ is modeled according to Equation 5a, with the exception of cases in which the channel i radiances in the 9 FOV's are all "thought to be unaffected by clouds". In these cases, $\widehat{A}_i$ is set equal to 1/3 and Equation 5b is used to model $\delta\widehat{R}_i$, because there should be no cloud-clearing errors in cases when all FOV's are clear as seen by channel i. The flaw in this methodology is that $\widehat{A}_i = 1/3$ indicates that the FOV's as seen by channel i are "thought to be clear", but that doesn't always imply that the FOV's are actually clear. Under some conditions with extensive stratus cloud cover, window channel observations are "thought to be clear" and, using Equation 5b, $\delta\widehat{R}_i$ is set equal to $1/3\ NE\Delta N_i$, when the scene is actually overcast and Equation 5a should have been used to obtain $\delta\widehat{R}_i$. When this situation occurs, a very poor retrieval results, especially with regard to lower tropospheric temperatures and surface skin temperature. The existence of a poor retrieval is reflected in large error estimates for lower tropospheric temperature as well as for total precipitable water, both of which terms are used in the generation of $\delta\widehat{R}_i^{\delta\eta}$. Therefore $\delta\widehat{R}_i$ would have been a very large number if Equation 5a were used in place of Equation 5b to generate $\delta\widehat{R}_i$. In addition to poor retrievals, very poor values of $\widehat{R}_i$ are also generated under these conditions for channels sensitive to the surface. Nevertheless, the QC flag for these bad values of $\widehat{R}_i$ is set equal to 0 because the use of Equation 5b to obtain $\widehat{R}_i$ results in a very small value for $\delta\widehat{\Theta}_i$, which is always less than the QC=0 threshold of 1K. This

situation does not occur often, but occurs much more often in V6 **AIRI2CCF** than in V6 **AIRS2CCF** O.

Unfortunately, not enough information is continued in the Level 2 cloud cleared data sets for the user to be able to generate the values of $\delta\widehat{R}_i$ that would have resulted if Equation 5a were used for these cases in place of Equation 5b. Nevertheless, there is a very easy way for the user to identify $\widehat{R}_i$ as having poor quality for these cases, which are characterized by a noise amplification factor (**CCfinal_Noise_Amp**) of 1/3, in that these cases are also characterized as having a surface skin temperature QC (**TSurfStd_QC**)=2. Note in Figure 2b that oceanic areas in which extensive low cloud cover exists are also marked by gaps in the spatial coverage of Tskin. Figure 5 shows otherwise analogous results to those shown in Figure 4, but using an additional test for $\delta\widehat{R}_i$ which says that if the noise amplification factor is 1/3 (that is, greater than 0.3333 and less than 0.3334), and the surface skin temperature has QC=2, then treat $\delta\widehat{R}_i$ as having QC=2. We applied this additional test to $\widehat{R}_i$ for all channels with $\nu > 740$ cm^{-1}, except for those in the 4.3 μm CO2 band between 2240 cm^{-1} and 2380 cm^{-1} that are not sensitive to surface emission, in the generation of the results shown in Figure 5.

Figure 5: Mean cloud-cleared radiance column brightness temperature, yield and bias 740 cm^{-1} to 2665 cm^{-1} for V6, QC=0 and filtered by CCfinal_Noise_Amp and TSurfStd_QC

The results shown in Figure 5 are almost identical to those in Figure 4 with regard to yield, but markedly different in the longwave and shortwave window regions with regard to both the standard deviation and the bias of the "errors" in $\widehat{\Theta}_i$. Now, the difference in the results between V6 AIRS+AMSU (**AIRI2CCF**) and V6 AIRS-Only (**AIRS2CCF**) is small, and as expected, V6 **AIRI2CCF** actually performs somewhat better than V6 **AIRS2CCF**. Taken at face value, the results shown in Figure 5 are still somewhat disturbing in that there appears to be a small negative bias, on the order of 0.5K, between $\widehat{\Theta}_i$ and Θ_i^{truth} over ocean in both the 11 μm and 3.7 μm window regions.

There are two possible contributions to this bias:
  1) cloud clearing in the window regions in general underestimate the effects of clouds on $R_{i,k}$, and hence $\widehat{\Theta}_i$ is in general too cold; or
  2) the bias between $\widehat{\Theta}_i$ and Θ_i^{truth} actually results from Θ_i^{truth} being in general too warm.

We conducted an experiment which generated analogous statistics only for ocean cases in which $\widetilde{A} = 1/3$ and Tskin had QC values of 0 or 1. These cases were both thought to be clear and were most likely actually clear, implying that there should be no cloud clearing errors for this ensemble of cases. We found the same -0.5K bias in $\left(\widehat{\Theta}_i - \Theta_i^{truth}\right)$ in both window spectral regions. The implication of this experiment is that $\widehat{\Theta}_i$ is in fact essentially unbiased and Θ_i^{truth} is 0.5K too high over ocean in window regions. This bias in Θ_i^{truth} could easily be the result of a very small overestimation of the ocean surface emissivity in the JPL emissivity model.

We strongly recommend that the user apply this additional test when assessing the utility of $\widehat{R}_i$ for scientific studies. The two appropriate words needed for the additional test are **CCfinal_Noise_Amp** and **TSurfStd_QC**. The first is included in the L2 Cloud Cleared Radiance Product (**AIRI2CCF**, **AIRH2CCF** and **AIRS2CCF**); the second must be accessed in the L2 Standard Product (**AIRX2RET**, **AIRH2RET** and **AIRS2RET**).

5 REFERENCES

Susskind, J., Barnet, C.D., and Blaisdell, J.M. (2003), "Retrieval of atmospheric and surface parameters from AIRS/AMSU/HSB data in the presence of clouds," *IEEE Trans. Geoscience and Remote Sensing*, **41**, 390-409, doi: 10.1109/TGRS.2002.808236.